



An association between the inferior humeral head osteophyte and teres minor fatty infiltration: evidence for axillary nerve entrapment in glenohumeral osteoarthritis

Peter J. Millett, MD, MSc^{a,*}, Jean-Yves Schoenahl, MD^a,
Matthew J. Allen, VetMB, PhD^b, Tatiana Motta, DVM, MSc^b, Trevor R. Gaskill, MD^a

^aSteadman Philippon Research Institute, Vail, CO, USA

^bDepartment of Veterinary Clinical Sciences, College of Veterinary Medicine, The Ohio State University, Columbus, OH, USA

Background: Glenohumeral osteoarthritis often results in inferior humeral osteophytes. Anatomic studies suggest that the axillary neurovascular bundle is in close proximity to the glenohumeral capsule. We therefore hypothesize that an inferior humeral osteophyte of sufficient magnitude could encroach on the axillary nerve and result in measurable fatty infiltration of the teres minor muscle.

Materials and methods: Preoperative magnetic resonance imaging studies of 91 consecutive arthritic shoulders were retrospectively reviewed. Two cohorts were established based on the presence of a humeral osteophyte. The distances from the axillary neurovascular bundle to various osseous structures were measured using calibrated software. Objective quantitative measurements of the degree of fatty infiltration of the teres minor muscles were obtained with image analysis software. Results were compared between cohorts.

Results: The distance between the inferior humerus and axillary neurovascular bundle was inversely correlated to the size of the inferior humeral osteophyte ($\rho = -0.631$, $P < .001$). Fatty infiltration of the teres minor was greater when an inferior osteophyte was present (11.9%) than when an osteophyte was not present (4.4%) ($P = .004$). A statistically significant correlation between the size of the humeral head spur and quantity of fat in the teres minor muscle belly ($\rho = 0.297$, $P = .005$) was identified.

Conclusion: These data are consistent with our hypothesis that the axillary nerve may be entrapped by the inferior humeral osteophyte often presenting with glenohumeral osteoarthritis. Entrapment may affect axillary nerve function and lead to changes in the teres minor muscle. Axillary neuropathy from an inferior humeral osteophyte may represent a contributing and treatable cause of pain in patients with glenohumeral osteoarthritis.

Level of evidence: Level III, Case-Control Study, Epidemiology Study.

© 2013 Journal of Shoulder and Elbow Surgery Board of Trustees.

Keywords: Humeral osteophytes; goat's beard; teres minor fatty infiltration; axillary neurovascular bundle

Glenohumeral osteoarthritis (GHOA) is characterized by pain, weakness, and cartilage degeneration. In some circumstances, a large inferior humeral osteophyte (goat's beard deformity) may develop, extending into the inferior glenohumeral joint capsule. Considering the intimate relationship of the axillary nerve to the inferior glenohumeral joint capsule, it is plausible that large humeral osteophytes may place the axillary nerve at risk for injury.^{2,4,16,22,27}

The axillary nerve provides motor innervation to the deltoid and teres minor muscles and is critical for normal shoulder function. It also carries sensory fibers from the lateral shoulder and innervates portions of the glenohumeral capsule.⁶⁻⁸ As exemplified by quadrilateral space syndrome, compression of the axillary neurovascular bundle can contribute to posterolateral shoulder pain and motor dysfunction.^{1,9,23,25} Many patients with GHOA also complain of lateral and posterior shoulder pain. Therefore, axillary nerve injury as a result of osteophytic spurring in patients with GHOA may manifest as posterior shoulder pain clinically or as fatty infiltration of distally innervated musculature on imaging modalities.^{12,17}

It is unclear, however, whether the neurovascular bundle is displaced as the inferior osteophyte grows or whether the osteophyte encroaches on the fixed neurovascular bundle to produce irritation. Therefore, the purpose of this study was to compare the proximity of the axillary neurovascular bundle to the inferior humerus in arthritic cohorts in the presence or absence of humeral osteophytes. Furthermore, teres minor fatty infiltration, serving as a surrogate marker of axillary nerve dysfunction, will be quantified. These factors will then be correlated with the presence and size of the inferior humeral osteophytes. Our hypothesis was that glenohumeral osteophytes are capable of encroaching on the axillary nerve and, if of sufficient magnitude, may result in axillary nerve dysfunction. This dysfunction will in turn be manifested as an increase in the degree of fatty infiltration within the teres minor muscle.

Anatomic considerations

The axillary neurovascular bundle includes the axillary nerve and the posterior humeral circumflex artery and vein. The posterior humeral circumflex artery arises from the axillary artery at the lower border of the subscapularis and runs posteriorly with its accompanying vein through the quadrilateral space. It winds around the neck of the humerus before anastomosing with the anterior humeral circumflex artery.

The axillary nerve arises from the posterior cord of the brachial plexus and passes beneath the coracoid process. From this location, it travels inferior to the subscapularis, running along the inferior joint capsule to enter the quadrilateral space.¹⁰ Two branches are formed near the long head of the triceps insertion. The anterior branch courses around the neck of the humerus and innervates the middle and anterior deltoid. The posterior branch is responsible for

posterior deltoid innervation, the teres minor motor branch, and the superior-lateral brachial cutaneous nerve. This cutaneous nerve provides sensory innervation to the lateral deltoid.^{4,8} The axillary nerve is tethered within the quadrilateral space, placing it at risk for injury after glenohumeral dislocation or humeral head fracture.^{5,6,21}

It is established that the course of the axillary nerve brings it in close proximity to the inferior glenohumeral capsule and is at risk during both open and arthroscopic shoulder procedures. Cadaveric studies suggest that the neurovascular bundle lies within 10 to 25 mm of the inferior glenoid rim.^{2,4,16,22,27} Its proximity to the inferior capsular recess, however, is much closer. As suggested by Bryan et al,⁷ the proximity of the axillary nerve to the capsule in this location may be 3.2 mm or less and is closest to the glenoid near the 5:30 to 6-o'clock position as it travels beneath the glenohumeral joint.^{4,8,11,14,15,22,27} Price et al²² reported that the motor branch to the teres minor muscle is reliably closest to the inferior joint capsule in this position. Therefore, this branch may be most susceptible to compressive disorders originating from the glenohumeral joint.

Materials and methods

Patient selection

A retrospective review identified all patients diagnosed with primary GHOA at our institution and treated by a single senior surgeon (P.J.M.) between 2005 and 2010. Considering that teres minor tears, shoulder dislocation, and previous instability surgery have been identified as possible etiologies for axillary nerve injury or teres minor fatty infiltration, we excluded subjects exhibiting these characteristics by history, by magnetic resonance imaging (MRI), or at the time of surgery from the study.^{2,3,13,14,18,22,24,26}

A total of 81 patients (98 shoulders) with primary GHOA were identified using our study criteria. Seven shoulders were excluded because the MRI study was of insufficient quality to allow fatty infiltration quantification by the image analysis software. The remaining 91 shoulders were then divided into 2 separate cohorts based on the presence of an inferior humeral osteophyte. A humeral osteophyte was present in 48% of the shoulders (44 of 91), and these shoulders comprised group I. No osteophytes were present in the remaining 52% (47 of 91), and these shoulders were therefore assigned to group II.

Radiographic measurements

Preoperative MRI studies were used to obtain all anatomic measurements. For each patient, the coronal-oblique T1 or proton density-weighted image was selected, located at the 6-o'clock position of the glenoid in the parasagittal plane (Fig. 1). Six measurements were obtained on each image using a calibrated measurement system (OfficePACS Power viewer; Stryker, Flower Mound, TX, USA). Distances were measured to the nearest portion of the neurovascular bundle.

The humeral head diameter (HHD) along the anatomic neck was measured, and the inferior glenoid osteophyte and humeral

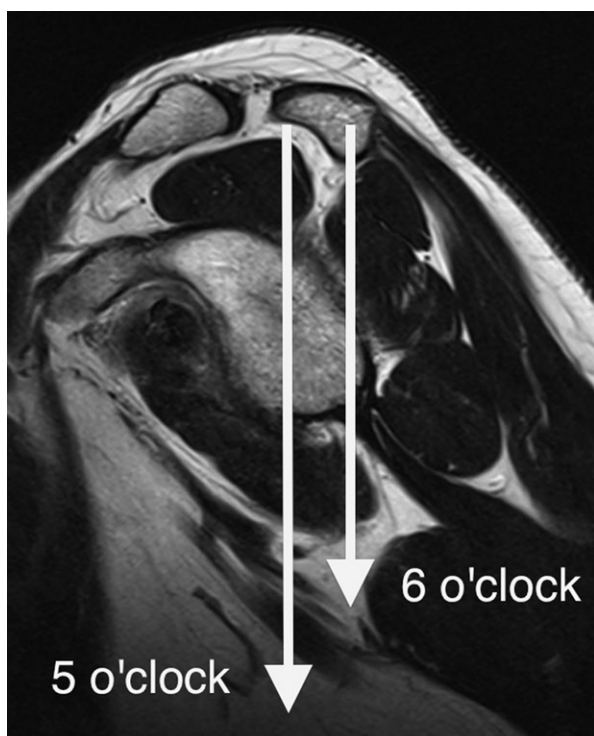


Figure 1 Parasagittal view used to select coronal oblique views from the 6-o'clock position.

head osteophyte were measured if present (Fig. 2). Osteophyte measurements were made from the junction of the osteophyte and native humeral head (or glenoid) to the inferior extent of the osteophyte. Distances were also measured from the neurovascular bundle to the middle of the glenoid (mid-glen) (Fig. 3) and the nearest portion of the glenoid or humerus (DH). When osteophytes were present, distances were measured to the nearest point of the respective osteophyte (Fig. 4).

To account for differences in patient size and gender, ratios were calculated by dividing each measured distance (distance from neurovascular bundle to middle of glenoid, distance to nearest portion of glenoid, and DH) by the HHD. A measurement reliability analysis was also completed. Each measurement was repeated on a sample of 25 patients 3 months after initial measurements were made, and intraclass correlation coefficients were calculated.

Fat percent assessment

MRI studies of each patient were evaluated for fatty infiltration of each rotator cuff muscle. The teres minor was selected as the primary surrogate for axillary nerve compression because the proximity of the branch to the teres minor has been established to be the closest to the inferior glenohumeral capsule.²² To objectively determine the amount of fatty tissue in each muscle, imaging analysis software (Mimics, version 13; Materialise, Plymouth, MI, USA) was used. A single researcher, blinded to patient information, selected each muscle on 8 consecutive sagittal magnetic resonance images using a lasso tool. The volume of fat and muscle was then quantified based on grayscale thresholds (Fig. 5). Fatty infiltration was ultimately calculated as the volume

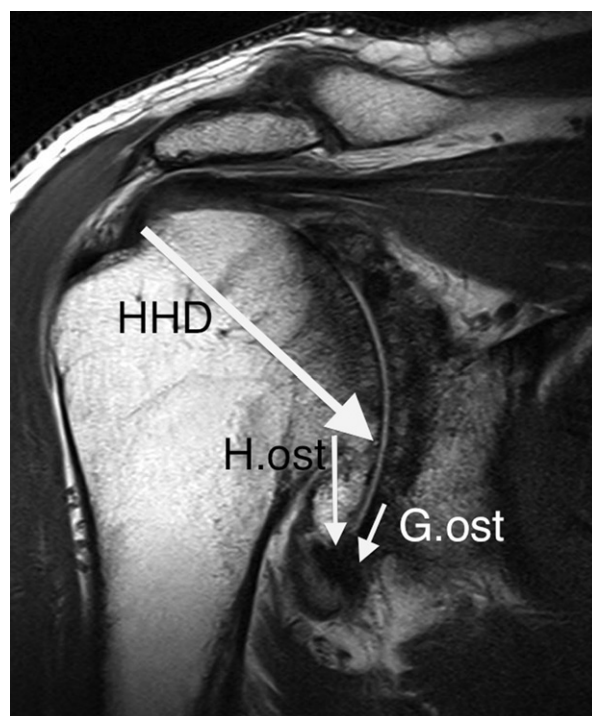


Figure 2 Representative image showing measurement of HHD and sizing of humeral head osteophyte (H.ost) and glenoid osteophyte (G.ost).

of fat divided by the total calculated muscle volume averaged over all images.

Statistical analysis

Student *t* tests were used to compare mean distances calculated for each group. Spearman correlation coefficients were used for nonparametric correlations. Differences between groups were considered significant at $P < .05$.

Results

The study population comprised 91 arthritic shoulders in 81 patients. Of the shoulders, 33 were in women and 58 in men. The mean age of each group at the time of MRI was 61 years (range, 21-85 years).

The intraclass correlation coefficient κ ranged between 0.84 and 1.00 for the imaging measurements taken separately 3 months apart. The mean HHD was 42 mm (range, 30-52 mm) and 45 mm (range, 34-56 mm) at the 6-o'clock position in cohorts I and II, respectively. A statistically significant difference in HHD between the 2 cohorts was found ($P = .001$). Humeral head osteophytes were present in 48% of arthritic shoulders (44 of 91) and averaged 12 mm (range, 0-24 mm) in size. Glenoid osteophytes were present in 5.5% of arthritic shoulders (5 of 91) and averaged 10 mm in size.

Mid-glenoid (mid-glen, mid-glen/HHD) measurements were similar between groups (Table I). The distance (DH)



Figure 3 Representative image showing measurement of the distance between the middle of the glenoid (MID-glen) and the axillary neurovascular bundle.



Figure 4 Representative image showing measurement of the distance from the tip of the glenoid (DG) and humeral head osteophyte (DH) to the axillary neurovascular bundle.

and distance ratio (DH/HHD) between the humeral head or inferior spur and neurovascular bundle was significantly ($P < .001$) smaller in shoulders where an inferior humeral osteophyte was identified (Table II, Fig. 6). This distance averaged 17 mm (range, 3-34 mm) in group I and 23 mm (range, 11-35 mm) in group II. The neurovascular bundle distance and humeral head osteophyte size were inversely correlated in the GHOA group ($\rho = -0.631$, $P < .001$).

Quantification of fatty infiltration

Fatty infiltration of the teres minor muscle was assessed in 91 arthritic shoulders. Overall, the mean percentage of fat in the teres minor muscle was 8.1% (range, 0.06%-76.2%) for the 91 included shoulders. An inferior humeral head osteophyte was present in 48% (44 of 91), and these shoulders comprised group I. The osteophyte averaged 12 mm in greatest dimension. The percentage of fatty infiltration was 9.7% (range, 0.10%-76.1%) in the presence of an inferior humeral osteophyte and 4.4% (range, 0.06%-40.8%) when no osteophyte was present ($P = .048$).

The size of the inferior humeral head osteophyte was correlated to the percentage of fat identified in the teres minor muscle ($\rho = 0.297$, $P = .005$). Similar associations could not be identified between the remaining rotator cuff muscles (non-axillary nerve innervated) and the humeral osteophyte or fatty infiltration of the teres minor. Age was also significantly correlated to percent fat in the teres minor

muscle ($\rho = 0.258$, $P = .015$). The distance measured between the neurovascular bundle and the humeral head was inversely correlated to the magnitude of teres minor fatty infiltration, but this failed to reach the significance threshold ($\rho = -0.115$, $P = .287$). Multivariate analysis showed that statistically significant independent predictors of teres minor fatty infiltration were spur size and age ($r = 0.23$, $P = .02$).

Discussion

This study indicates that the distance to the axillary neurovascular bundle was smaller in the presence of humeral osteophytes as compared with non-osteophytic arthritic controls. Moreover, the distance between the humerus and neurovascular bundle decreased as osteophyte size increased. Thus, large humeral osteophytes may be capable of encroaching on the axillary neurovascular bundle. This series also showed that as osteophyte size increased, the magnitude of teres minor fatty infiltration also grew. Therefore, in this cohort, the presence and size of the inferior humeral osteophyte were directly correlated with the quantity of fat in the teres minor muscle.

The distance between the glenoid (inferior rim and mid glenoid) and the axillary neurovascular bundle was similar between groups. Therefore, it appears that the inferior humeral osteophytes do not displace the axillary

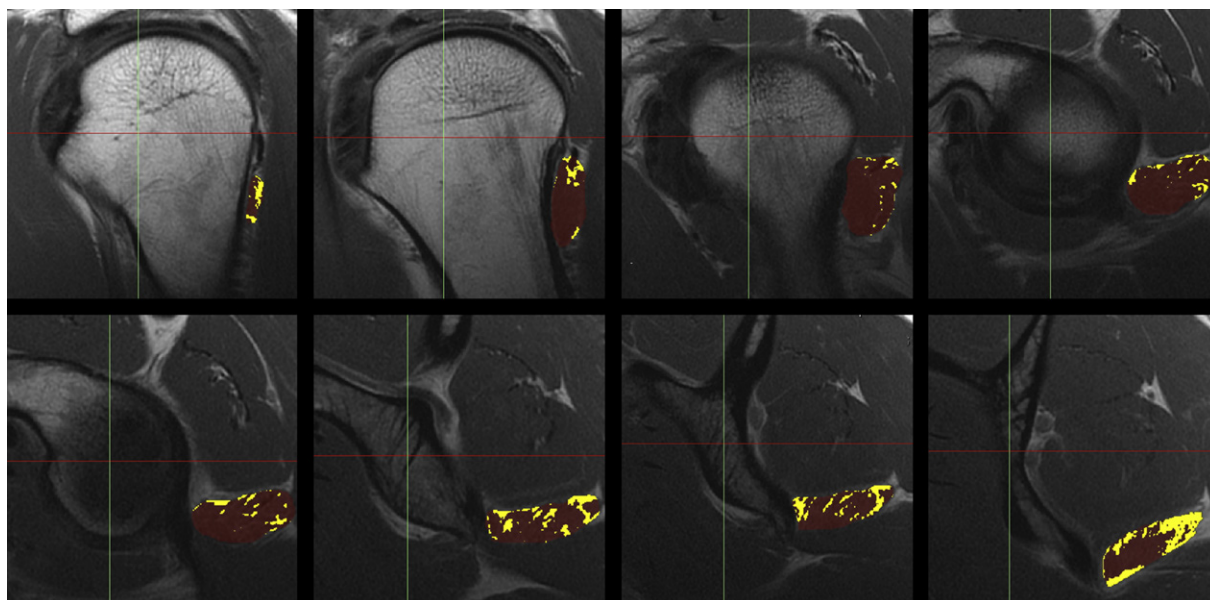


Figure 5 Eight representative parasagittal magnetic resonance images of a left shoulder depicting the calculation of muscular fatty infiltration by the image analysis software. Muscle fibers are colored in burgundy and yellow represents fat. The fat signal is then divided by the muscular volume and averaged between each image.

Table I Absolute distance measured from mid glenoid and distance ratio to axillary neurovascular bundle for osteophytic and non-osteophytic groups

	Osteophytic group (group I) (n = 44)	Non-osteophytic group (group II) (n = 47)
Distance measured from mid glenoid at 6-o'clock position (mm)	33.6 ($P = .001$)	29.7
Mid-glenoid distance/HHD at 6-o'clock position	0.74 ($P = .270$)	0.72

Table II Distance measured from humeral head or inferior humeral osteophyte and distance ratio to axillary neurovascular bundle for non-osteophytic and osteophytic groups

	Osteophytic group (group I) (n = 44)	Non-osteophytic group (group II) (n = 47)
DH at 6-o'clock position (mm)	16.8 ($P < .001$)	22.7
DH/HHD at 6-o'clock position	0.37 ($P < .001$)	0.55

neurovascular bundle with respect to the glenoid. Rather, the decreased distance between the humerus and neurovascular bundle identified in the presence of osteophytes occurs because the humeral osteophyte encroaches on the neurovascular bundle. Conversely, the axillary neurovascular bundle does not seem to displace or adapt to the bony changes that occur as the goat's beard deformity develops. This may increase its susceptibility to compression.

Most traumatic axillary nerve injuries occur due to a traction-type mechanism.^{2,3,24,26} Alternatively axillary nerve compression due to mass effect has been described in cases of neoplasia, hypertrophied musculature, and malunited scapular fractures.^{1,23,25} A large humeral osteophyte could potentially result in a similar compressive injury to the axillary nerve. Analogous to quadrilateral space syndrome, the clinical manifestation of this injury would likely include posterior and lateral shoulder pain and potentially fatty

infiltration of the teres minor muscle. Considering that the motor branch to the teres minor is reliably closest to the glenohumeral joint, it seems plausible that it may be most at risk from large humeral head osteophytes.²²

To this end, patients with GHOA often present with posterior and lateral shoulder pain. In cohorts of young patients who are not optimal candidates for glenohumeral arthroplasty, we have seen considerable symptomatic improvement after arthroscopic humeral osteoplasty and axillary nerve neurolysis.^{19,20} Whereas the long-term results of this procedure remain to be defined, comprehensive arthroscopic management of glenohumeral arthrosis (Comprehensive Arthroscopic Management [CAM] procedure)^{19,20} may provide a window for-improved function and pain relief in young, high-demand patients who wish to avoid glenohumeral arthroplasty. This is a technically demanding procedure and should only be performed by experienced shoulder arthroscopists.^{19,20}

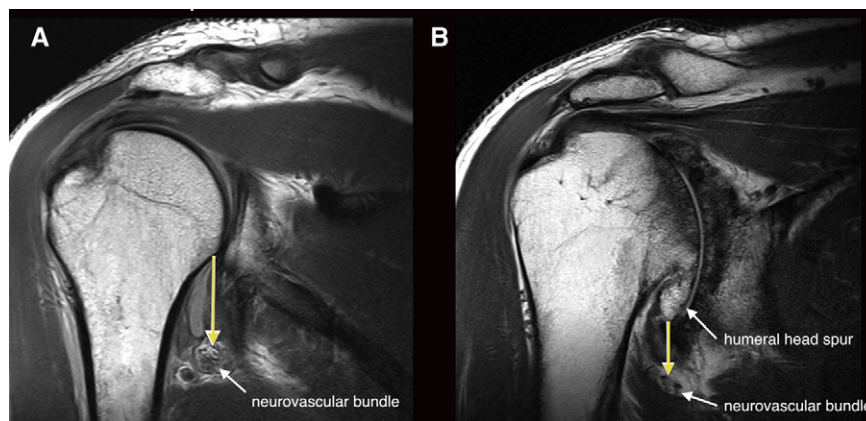


Figure 6 Representative MRI images of a right shoulder in the absence (a) and presence (b) of an inferior osteophyte. Note the decreased distance (arrow) between the humerus and neurovascular bundle.

There are several limitations to this analysis. First, the field strength of reviewed MRI studies was not standardized, and lower-field strength scanners may contribute to decreased image resolution and increased measurement error. We believe that this possibility is minimized because all MRI studies were obtained with either a 1.5-T or 3.0-T scanner.

It is established that axillary nerve compression can result in teres minor fatty infiltration when disorders such as quadrilateral space syndrome are present.^{1,9,23,25} By contrast, however, it remains unclear whether teres minor fatty infiltration is a robust surrogate for axillary nerve entrapment in the setting of glenohumeral arthrosis. Our study indicates that an association between humeral osteophytes and teres minor fatty infiltration is present in this setting. It is important to note, however, that although this series indicates that axillary compression by humeral osteophytes is plausible, further investigation is necessary to establish causation.

Moreover, it is likely that stiffness and disuse atrophy present in arthritic shoulders will result in some degree of global fatty infiltration of the rotator cuff. Although we would expect these factors to affect all rotator cuff muscles equally, analysis of the remaining rotator cuff muscles (not innervated by the axillary nerve) did not show an association between fatty infiltration of these muscles and the teres minor. Whereas this suggests that stiffness or disuse atrophy is unlikely to be the etiology of the identified teres minor fatty infiltration, it remains unclear whether such conditions are capable of resulting in isolated teres minor fatty infiltration.

Finally, arm position has been known to influence the location of the neurovascular bundle. Although all patients underwent MRI with the arm in adduction and neutral rotation, it was unclear what effect small differences in arm position across patients may have had on the outcomes. In addition, only static measurements can be made on magnetic resonance images. Therefore, this study cannot confirm any dynamic interaction that could cause nerve

impingement or stretching beneath the humeral head osteophyte in various shoulder positions.

Conclusion

The data from this study were consistent with our hypothesis that humeral osteophytes are capable of encroaching on the axillary neurovascular bundle and are associated with fatty infiltration of the teres minor muscle. Fatty infiltration of the teres minor was correlated with the presence and size of inferior humeral osteophytes. Therefore, it may be reasonable to hypothesize that humeral osteophytes are capable of causing axillary nerve injury if they become of sufficient size. Arthroscopic decompression through a humeral osteoplasty (spur removal) in addition to joint debridement and capsular release may be a reasonable option for young patients with large osteophytes as a joint preservation technique.^{19,20} Additional basic science and clinical studies are needed to evaluate the efficacy of this procedure and to determine whether changes identified in this series are reversible.

Disclaimer

Dr Millett is a consultant for and receives payments from Arthrex and has stock options in Game Ready, which are related to the subject of this work. Dr Millett also receives support from the Steadman Philippon Research Institute. Companies that support the Steadman Philippon Research Institute include Arthrex, Össur, Smith & Nephew, ArthroCare, OrthoRehab, and Siemens.

Dr Schoenahl receives support from the Steadman Philippon Research Institute.

The other authors, their immediate families, and any research foundations with which they are affiliated have not received any financial payments or other benefits from any commercial entity related to the subject of this article.

References

- Amin MF, Berst M, el-Khoury GY. An unusual cause of the quadrilateral space impingement syndrome by a bone spike. *Skeletal Radiol* 2006;35:956-8. <http://dx.doi.org/10.1007/s00256-006-0092-6>
- Apaydin N, Tubbs RS, Loukas M, Duparc F. Review of the surgical anatomy of the axillary nerve and the anatomic basis of its iatrogenic and traumatic injury. *Surg Radiol Anat* 2010;32:193-201. <http://dx.doi.org/10.1007/s00276-009-0594-8>
- Aval SM, Durand P Jr, Shankwiler JA. Neurovascular injuries to the athlete's shoulder: part II. *J Am Acad Orthop Surg* 2007;15:281-9.
- Ball CM, Steger T, Galatz LM, Yamaguchi K. The posterior branch of the axillary nerve: an anatomic study. *J Bone Joint Surg Am* 2003;85:1497-501.
- Bateman JE. Nerve injuries about the shoulder in sports. *J Bone Joint Surg Am* 1967;49:785-92.
- Bonnard C, Anastakis DJ, van Melle G, Narakas AO. Isolated and combined lesions of the axillary nerve. A review of 146 cases. *J Bone Joint Surg Br* 1999;81:212-7.
- Bryan WJ, Schauder K, Tullos HS. The axillary nerve and its relationship to common sports medicine shoulder procedures. *Am J Sports Med* 1986;14:113-6.
- Burkhead WZ, Scheinberg RR, Box G. Surgical anatomy of the axillary nerve. *J Shoulder Elbow Surg* 1992;1:31-6.
- Cahill BR, Palmer RE. Quadrilateral space syndrome. *J Hand Surg Am* 1983;8:65-9.
- Duparc F, Bocquet G, Simonet J, Freger P. Anatomical basis of the variable aspects of injuries of the axillary nerve (excluding the terminal branches in the deltoid muscle). *Surg Radiol Anat* 1997;19:127-32.
- Eakin CL, Dvirnak P, Miller CM, Hawkins RJ. The relationship of the axillary nerve to arthroscopically placed capsulolabral sutures. An anatomic study. *Am J Sports Med* 1998;26:505-9.
- Engel WK, Brooke MH, Nelson PG. Histochemical studies of denervated or tenotomized cat muscle: illustrating difficulties in relating experimental animal conditions to human neuromuscular diseases. *Ann N Y Acad Sci* 1966;138:160-85.
- Gerber C, Meyer DC, Schneeberger AG, Hoppeler H, von Rechenberg B. Effect of tendon release and delayed repair on the structure of the muscles of the rotator cuff: an experimental study in sheep. *J Bone Joint Surg Am* 2004;86:1973-82.
- Loomer R, Graham B. Anatomy of the axillary nerve and its relation to inferior capsular shift. *Clin Orthop Relat Res* 1989;243:100-5.
- McCarty EC, Warren RF, Deng XH, Craig EV, Potter H. Temperature along the axillary nerve during radiofrequency-induced thermal capsular shrinkage. *Am J Sports Med* 2004;32:909-14. <http://dx.doi.org/10.1177/0363546503260064>
- McFarland EG, Caicedo JC, Kim TK, Banchasuek P. Prevention of axillary nerve injury in anterior shoulder reconstructions: use of a subscapularis muscle-splitting technique and a review of the literature. *Am J Sports Med* 2002;30:601-6.
- McMinn R, Vrbova G. Morphological changes in red and pale muscles following tenotomy. *Nature* 1966;195:509.
- Meyer DC, Hoppeler H, von Rechenberg B, Gerber C. A pathomechanical concept explains muscle loss and fatty muscular changes following surgical tendon release. *J Orthop Res* 2004;22:1004-7. <http://dx.doi.org/10.1016/j.orthres.2004.02.009>
- Millett PJ, Gaskill TR. Arthroscopic management of glenohumeral arthrosis: humeral osteoplasty, capsular release, and arthroscopic axillary nerve neurolysis as a joint-preserving approach. *Arthroscopy* 2011;27:1296-303. <http://dx.doi.org/10.1016/j.arthro.2011.03.089>
- Millett PJ, Gaskill TR. Arthroscopic trans-capsular axillary nerve decompression: indication and surgical technique. *Arthroscopy* 2011;27:1296-303. <http://dx.doi.org/10.1016/j.arthro.2011.05.003>
- Petrucci FS, Morelli A, Raimondi PL. Axillary nerve injuries—21 cases treated by nerve graft and neurolysis. *J Hand Surg Am* 1982;7:271-8.
- Price MR, Tillett ED, Acland RD, Nettleton GS. Determining the relationship of the axillary nerve to the shoulder joint capsule from an arthroscopic perspective. *J Bone Joint Surg Am* 2004;86A:2135-42.
- Robinson P, White LM, Lax M, Salonen D, Bell RS. Quadrilateral space syndrome caused by glenoid labral cyst. *AJR Am J Roentgenol* 2000;175:1103-5.
- Safran MR. Nerve injury about the shoulder in athletes, part 1: suprascapular nerve and axillary nerve. *Am J Sports Med* 2004;32:803-19. <http://dx.doi.org/10.1177/0363546504264582>
- Sanders TG, Tirman PF. Paralabral cyst: an unusual cause of quadrilateral space syndrome. *Arthroscopy* 1999;15:632-7.
- Steinmann SP, Moran EA. Axillary nerve injury: diagnosis and treatment. *J Am Acad Orthop Surg* 2001;9:328-35.
- Yoo JC, Kim JH, Ahn JH, Lee SH. Arthroscopic perspective of the axillary nerve in relation to the glenoid and arm position: a cadaveric study. *Arthroscopy* 2007;23:1271-7. <http://dx.doi.org/10.1016/j.arthro.2007.07.011>